Journal of Engineering Mathematics, Vol. 15, No. 4, October 1981

On the wave resistance of a submerged semi-elliptical body

L. K. FORBES

Department of Applied Mathematics, University of Adelaide, Adelaide, Australia

(Received February 18, 1981)

SUMMARY

A numerical method is presented for determining the shape of the free surface of a running stream which is disturbed by a semi-elliptical body affixed to the bottom. The effects of non-linearity on the wave resistance experienced by the semi-ellipse are discussed; most importantly, it is shown that there exist ellipses for which the non-linear wave drag is zero. Two wave-free (drag-free) surface profiles are presented.

1. Introduction

This paper concerns the two-dimensional, steady flow of an ideal fluid in a horizontal stream, attached to the bottom of which is a semi-elliptical obstacle. Far upstream the fluid flow is uniform, whilst a regular train of waves is to be expected in general on the downstream side of the ellipse. The energy radiated away to infinity by this downstream wave train is exactly balanced by a horizontal force component (the wave resistance) acting on the ellipse. In this paper we aim to demonstrate that, for certain ellipse shapes, non-linear free-surface profiles are obtained which possess no waves on the downstream side, resulting in zero wave resistance experienced by the semi-elliptical body. This result may be of significance in the design of certain underwater craft, for example.

A linearized solution to the present problem was calculated by Lamb ([1], p. 409) and will be discussed in Section 3 of this paper. One of the features of this linearized solution is that, for a given value of the upstream Froude number, the free surface is predicted to be free of downstream waves for ellipses of certain special lengths, resulting in zero drag force acting on the ellipse in these cases. In fact, the plot of wave resistance *versus* ellipse length for fixed upstream Froude number and ellipse height is undulatory and passes through zero infinitely often, giving rise to a countably infinite set of ellipse lengths for which the wave resistance is zero, at each value of the upstream Froude number.

The question of whether a wave-making disturbance may ever give rise to a *non-linear* wave resistance of precisely zero has been investigated recently by Schwartz [2]. He considered the problem of waves induced in a fluid of infinite depth by a moving pressure distribution applied to the free surface, and demonstrated that, for certain values of the pressure length, the non-linear wave resistance obtained was indeed extremely small, with a value of the order of 10^{-5} times the maximum resistance obtained with the same value of non-dimensional overpressure. The corresponding problem for a fluid of fixed finite depth was considered by von Kerczek and

Salvesen [3]. Their results also appear to indicate very small values of wave resistance for certain pressure lengths.

In the present paper, the problem is formulated inversely, by allowing the velocity potential and streamfunction to be independent variables. The solution is obtained utilizing a boundary-integral technique; consequently, points in the numerical scheme need only be placed on the fluid boundaries, rather than throughout the entire region. In addition, the bottom is conformally mapped onto a straight line, so that it is now only necessary to place numerical grid points at the free surface, with the bottom condition being satisfied automatically in the boundary-integral formulation of the problem. This formulation ensures maximum computational efficiency in obtaining non-linear free-surface profiles.

2. Formulation of the problem

We consider two-dimensional, steady flow of an ideal fluid in a channel in which the flow infinitely far upstream is uniform, with depth H and velocity c. The fluid flows from left to right. A semi-elliptical object of length $2R_X$ and height R_Y is attached to the channel bed, which is otherwise flat and horizontal, and is placed symmetrically about the y-axis, which points vertically. The fluid is subject to the downward acceleration of gravity, g.

The problem is expressed in terms of dimensionless variables forthwith, by referencing all lengths and velocities to the quantities H and c respectively. The velocity potential ϕ and streamfunction ψ are non-dimensionalized with respect to the quantity cH; in terms of dimensionless variables, the bottom is chosen to be the streamline $\psi = 0$, and the free surface is thus $\psi = 1$. Solutions to this problem are thus dependent upon the three dimensionless parameters

$$F = \frac{c}{(gH)^{\frac{1}{2}}}, \quad \alpha = \frac{R_X}{H} \quad \text{and} \quad \beta = \frac{R_Y}{H}.$$

The quantity F is the upstream depth-based Froude number, and α and β are respectively the dimensionless ellipse half-length and the ellipse height. The non-dimensional flow situation is depicted in Fig. 1.

Since the fluid is incompressible and flows without rotation, it follows that the velocity potential and streamfunction obey the Cauchy-Riemann equations in the fluid interior. Thus the complex function $f = \phi + i\psi$ is to be sought as an analytic function of the variable $z = x + iy$.

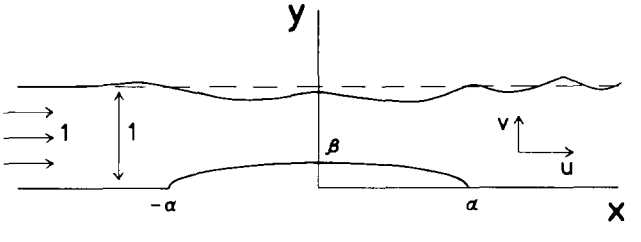

Figure 1. The non-dimensional flow situation in the z-plane.

The motion of the fluid at the free surface is governed by the Bernoulli equation

$$\tfrac{1}{2}F^2 w\bar{w} + y = \tfrac{1}{2}F^2 + 1, \tag{1}$$

where

$$w = \frac{df}{dz} = u - iv,$$

and u,v are the horizontal and vertical components of velocity. The bar denotes complex conjugation. The condition of no flow normal to the bottom is expressed as

$$u\frac{dh}{dx} = v \quad \text{on} \quad y = h(x) \tag{2a}$$

where the bottom $y = h(x)$ is described by the equation

$$h(x) = \begin{cases} 0, & |x| \geqslant \alpha \\ \dfrac{\beta}{\alpha}(\alpha^2 - x^2)^{\frac{1}{2}}, & |x| \leqslant \alpha. \end{cases} \tag{2b}$$

For the purposes of numerical computation, the problem formulated in the z-plane, defined by equations (1) and (2), is now transformed into a τ-plane in which the bottom streamline becomes a straight line. This avoids the potential difficulties associated with the stagnation points at $x = \pm\alpha$. (see Forbes and Schwartz [4]). The new variable $\tau = \xi + i\eta$ is defined by the relation

$$z = \tau + \frac{\beta}{\alpha}(\tau^2 - \alpha^2)^{\frac{1}{2}}, \tag{3}$$

which is a straightforward generalization of the Joukowski transformation used in [4]. Note that the bottom condition in the τ-plane becomes simply

$$Im\left\{\frac{df}{d\tau}\right\} = 0 \quad \text{on} \quad \eta = 0.$$

It is convenient at this stage to interchange the roles of τ and f, seeking to solve for $\tau = \xi + i\eta$ as an analytic function of the independent variable $f = \phi + i\psi$. This considerably simplifies the problem, for although the location of the free surface is unknown in the τ-plane, in the f-plane it has the known location $\psi = 1$. In addition, the kinematic free-surface condition is satisfied identically in the f-plane. The bottom condition takes the form

$$\eta = 0 \quad \text{on} \quad \psi = 0, \tag{4}$$

and the Bernoulli equation at the free surface becomes

$$\tfrac{1}{2}F^2 \frac{\alpha^2(A^2+B^2)}{(\alpha A+\beta\xi)^2+(\alpha B+\beta\eta)^2}\frac{1}{\tau_\phi\bar{\tau}_\phi}+\eta+\frac{\beta}{\alpha}B=\tfrac{1}{2}F^2+1 \quad \text{on} \quad \psi=1, \tag{5}$$

where we have defined

$$(\tau^2-\alpha^2)^{\frac{1}{2}}=A+iB,$$

and the subscripts denote partial differentiation. Far upstream, the flow is uniform, which results in the radiation condition

$$\tau\to f\left(1+\frac{\beta}{\alpha}\right)^{-1} \quad \text{as} \quad \phi\to-\infty. \tag{6}$$

The Bernoulli equation (5) provides one relation between ξ and η at the free surface; in order that both these functions may be found there, a second relation between them must be obtained. To do this, the f-plane strip $0\leqslant\psi\leqslant 1$ is first extended by Schwarz reflection about the bottom $\psi=0$. The satisfaction of the bottom condition (4) then requires that values of the derivative τ' on the image strip $-1\leqslant\psi\leqslant 0$ be related to values on the true strip $0\leqslant\psi\leqslant 1$ by the reflection formula

$$\tau'(\bar{f})=\bar{\tau}'(f). \tag{7}$$

Cauchy's Integral theorem is now applied to the analytic function

$$\chi(f)=\tau'(f)-\left(1+\frac{\beta}{\alpha}\right)^{-1}$$

on a rectangular path consisting of the free surface $\psi=1$ and its image $\psi=-1$ connected by vertical lines at $\phi\to\pm\infty$. For a point $f=\phi+i\psi$ within the path of integration, this yields

$$\chi(f)=\frac{1}{2\pi i}\left\{-\int_{-\infty}^{\infty}\frac{\chi(\theta+i)\,d\theta}{\theta+i-f}+\int_{-\infty}^{\infty}\frac{\chi(\theta-i)\,d\theta}{\theta-i-f}\right\}. \tag{8}$$

The desired relation between the real and imaginary parts of $\tau'(f)$ at the free surface is obtained by allowing f to become a point on the true free surface $\psi=1$, and deforming the path of integration about this point in a semi-circle of vanishingly small radius. Values of $\tau'(f)$ at the image surface $\psi=-1$ are now eliminated in favour of values at the true surface $\psi=1$, by means of equation (7). Finally, on taking real parts, we obtain

$$\left[\xi_\phi(\phi,1)-\left(1+\frac{\beta}{\alpha}\right)^{-1}\right]-\frac{2}{\pi}\int_{-\infty}^{\infty}\frac{d\theta}{(\theta-\phi)^2+4}\left[\xi_\theta(\theta,1)-\left(1+\frac{\beta}{\alpha}\right)^{-1}\right]=$$

$$=-\frac{1}{\pi}\left\{\int_{-\infty}^{\infty}\frac{\eta_\theta(\theta,1)\,d\theta}{\theta-\phi}+\int_{-\infty}^{\infty}\frac{\eta_\theta(\theta,1)(\theta-\phi)\,d\theta}{(\theta-\phi)^2+4}\right\}. \tag{9}$$

The free-surface profile is thus found parametrically in the form $(\xi(\phi,1),\eta(\phi,1))$ by solving the system of equations (5), (6) and (9). The variables x and y may be recovered from equation (3).

The wave drag D is calculated by integrating the pressure p over the ellipse surface. Thus

$$D = \int_{-\alpha}^{\alpha} p\, h'(x)\, \mathrm{d}x = \tfrac{1}{2} F^2 \frac{\beta}{\alpha} \int_{-\alpha}^{\alpha} (u^2 + v^2) \frac{x}{(\alpha^2 - x^2)^{\frac{1}{2}}}\, \mathrm{d}x. \tag{10}$$

After being transformed into the τ-plane and finally into the f-plane, equation (10) becomes

$$D = \tfrac{1}{2} F^2 \frac{\beta}{\alpha} \int_{\phi_{-\alpha}}^{\phi_{+\alpha}} \frac{\xi}{\xi_\phi} \frac{(\alpha^2 - \xi^2)^{\frac{1}{2}}}{\left[\left(\frac{\beta}{\alpha}\right)^2 - 1\right] \xi^2 + \alpha^2}\, \mathrm{d}\phi, \tag{11}$$

where the function ξ in equation (11) is to be evaluated along $\psi = 0$, and the quantities $\phi_{\pm\alpha}$ are the solutions to the equations

$$\xi(\phi_{\pm\alpha}, 0) = \pm\alpha. \tag{12}$$

The pressure p and drag D are made dimensionless by reference to the quantities $\rho g H$ and $\rho g H^2$ respectively, where ρ is the density of the fluid.

3. A linearized theory

The linearized theory appropriate to this problem is derived by regarding β as a small parameter and expressing the solution $\tau(f)$ as a regular perturbation expansion in this quantity. Upon substituting into the flow equations and retaining only lowest order terms in β, a linear system of equations is obtained, which appears to be too difficult to solve in closed form. Accordingly, this theory will not be pursued further.

An alternative linearized theory, valid for ellipses with an aspect ratio β/α of order 1, may be derived after the fashion of Forbes and Schwartz [4]. This approach will not be described further here, although details are given in Forbes [5].

Yet another linearized approach is that adopted by Lamb ([1], p. 409). This theory assumes that the solution may be considered as a small perturbation to uniform flow; this assumption clearly does not hold in the vicinity of the stagnation points at $z = \pm\alpha$. For the solution $f(z)$, Lamb's theory gives

$$f = z - \beta \int_0^{\infty} \frac{J_1(\alpha\kappa)}{\kappa} \frac{\frac{1}{F^2} \sin(\kappa z - i\kappa) + i\kappa \cos(\kappa z - i\kappa)}{\kappa \cosh(\kappa) - \frac{1}{F^2} \sinh(\kappa)}\, \mathrm{d}\kappa. \tag{13}$$

The free-surface elevation may be obtained from Lamb ([1]), p. 410, eq. (8)). With the present choice of coordinate system, this becomes

$$y = 1 + \beta \int_0^\infty \frac{J_1(\alpha\kappa)\cos(\kappa x)}{\kappa\cosh(\kappa) - \frac{1}{F^2}\sinh(\kappa)}\, d\kappa. \tag{14}$$

The function J_1 appearing in equations (13) and (14) is the first kind Bessel function of order one.

When $F^2 > 1$, the flow is symmetric about the y-axis, and the free surface does not possess waves. For the critical value $F^2 = 1$, however, there is no solution, since the integrals in equations (13) and (14) are divergent due to a singularity in the integrands at $\kappa = 0$.

When $F^2 < 1$, there is a singularity in the paths of integration at $\kappa = \kappa_0$, where κ_0 is the positive real root of the transcendental equation

$$\tanh(\kappa_0) = F^2\kappa_0.$$

In this case, the interpretation of integrals of the type shown in equations (13) and (14) is well known, and is discussed extensively in the literature (see, for example, Wehausen and Laitone [6]). The integrals are considered to be contour integrals in the complex κ-plane, with the path of integration by passing the pole singularity at κ_0 in a semi-circle of vanishingly small radius. Thus the integral in equation (13) may be expressed as the Cauchy Principal Value of the same integrand plus the term

$$\frac{\pi J_1(\alpha\kappa_0)}{\kappa_0} \frac{\frac{1}{F^2}\cos(\kappa_0 z - i\kappa_0) - i\kappa_0\sin(\kappa_0 z - i\kappa_0)}{\left[1 + F^2\kappa_0^2 - \frac{1}{F^2}\right]\cosh(\kappa_0)}.$$

A similar result is obtained for the integral in equation (14).

Thus it is evident that the free surface possesses no waves far upstream for $F^2 < 1$; downstream of the semi-ellipse, however, is a uniform train of sinusoidal waves. Far downstream, equation (14) yields the free-surface profile

$$y \to 1 - A_1\sin(\kappa_0 x),$$

where the wave amplitude A_1 is given by

$$A_1 = \frac{2\pi\beta J_1(\alpha\kappa_0)}{\left[1 + \kappa_0^2 F^2 - \frac{1}{F^2}\right]\cosh(\kappa_0)} \tag{15}$$

The wave drag D may be calculated by substituting equation (13) into equation (10). This results in the classical formula

$$D = \tfrac{1}{4}A_1^2 \left[1 - \frac{2\kappa_0}{\sinh(2\kappa_0)} \right] + O(\beta^3), \tag{16}$$

which is given in Lamb ([1], p. 415).

A remarkable feature of this theory is that the wave amplitude A_1 and linearized wave resistance D may become zero. This occurs each time the ellipse halflength α takes the value

$$\alpha = \frac{j_{1,s}}{\kappa_0}, \quad s = 0, 1, ...,$$

where $j_{1,s}$ is the s-th zero of the Bessel function J_1.

4. Numerical methods

The system of equations (5), (6) and (9) is to be solved at the $N + 1$ equally-spaced surface points $\phi_0, \phi_1, ..., \phi_N$. To begin, the integrals in equation (9) are truncated upstream and downstream at the points ϕ_0 and ϕ_N, and the singularity is subtracted from the Cauchy Principal-Value integral, leaving a non-singular integral plus a natural logarithm term. The equation is now evaluated at the midpoints $\phi = \phi_{k-\frac{1}{2}}$, $k = 1, ..., N$ and the integrals are discretized using Simpson's Rule. Thus equation (9) is approximated by a matrix system of the form

$$\left[\xi'_{k-\frac{1}{2}} - \left(1 + \frac{\beta}{\alpha}\right)^{-1} \right] - \frac{2}{\pi} \sum_{j=0}^{N} a_{kj} \left[\xi'_j - \left(1 + \frac{\beta}{\alpha}\right)^{-1} \right] =$$

$$= -\frac{1}{\pi} \left\{ \sum_{j=0}^{N} b_{kj}(\eta'_j - \eta'_{k-\frac{1}{2}}) + \sum_{j=0}^{N} c_{kj}\eta'_j \right\} - \frac{1}{\pi} \eta'_{k-\frac{1}{2}} \ln \left(\frac{\phi_N - \phi_{k-\frac{1}{2}}}{\phi_{k-\frac{1}{2}} - \phi_0} \right),$$

$$k = 1, ..., N, \tag{17}$$

with suitable weights a_{kj}, b_{kj} and c_{kj}. A three-point interpolation formula, consistent with the parabolae fitted by Simpson's Rule, is used to express $\xi'_{k-\frac{1}{2}}$ and $\eta'_{k-\frac{1}{2}}$ in terms of values of these functions at neighbouring whole points, so that equation (17) becomes

$$\sum_{j=0}^{N} d_{kj} \left[\xi'_j - \left(1 + \frac{\beta}{\alpha}\right)^{-1} \right] = \sum_{j=0}^{N} e_{kj}\eta'_j, \quad k = 1, ..., N. \tag{18}$$

The radiation condition (6) is now imposed at $\phi = \phi_0$; the quantities ξ_0, η_0 and η'_0 are obtained

from equation (6), and Bernoulli's equation (5) then gives ξ_0'. Since these quantities are now all known, equation (18) may be inverted to yield

$$\xi_i' = \left(1 + \frac{\beta}{\alpha}\right)^{-1} + \sum_{j=1}^{N} H_{ij}\eta_j' + H_{j,N+1}\left[\xi_0' - \left(1 + \frac{\beta}{\alpha}\right)^{-1}\right] + H_{i,N+2}\eta_0',$$

$$i = 1, ..., N. \tag{19}$$

The functions ξ and η are obtained using the Gregory integration formula. Thus

$$\xi_i = \xi_0 + \sum_{j=0}^{N} w_{ij}\xi_j'$$

and

$$\eta_i = \eta_0 + \sum_{j=0}^{N} w_{ij}\eta_0', \quad i = 1, ..., N, \tag{20}$$

where the w_{ij} are appropriate weights.

The Bernoulli equation (5), evaluated at each of the N points $\phi_1, ..., \phi_N$, yields a system of N non-linear algebraic equations in the N unknowns $\eta_1', ..., \eta_N'$, after the quantities ξ_i', ξ_i, η_i, $i = 1, ..., N$ have been eliminated using equations (19) and (20). This system may be written

$$P_i(\eta_1', \eta_2', ..., \eta_N') = 0, \quad i = 1, ..., N, \tag{21}$$

where P_i denotes the pressure at the i-th free-surface point.

Equations (21) are solved by Newton's method. Thus, if the estimate at the k-th iteration is written $\eta_j'^{(k)}, j = 1, ..., N$, then the next estimate is obtained from the formula

$$\eta_j'^{(k+1)} = \eta_j'^{(k)} + \Delta_j^{(k)}, \quad j = 1, ..., N, \tag{22}$$

where the correction step $\Delta_j^{(k)}$ is the solution to the matrix equation

$$\sum_{j=1}^{N} \left[\frac{\partial P_i}{\partial \eta_j'}\right]^{(k)} \Delta_j^{(k)} = -P_i^{(k)}, \quad i = 1, ..., N.$$

The elements of the Jacobian matrix, $\partial P_i / \partial \eta_j'$, are obtained by exact differentiation of equation (21). If the vector $\eta_j'^{(k+1)}, j = 1, ..., N$ obtained from equation (22) is a *worse* estimate of the solution than $\eta_j'^{(k)}$ (in the sense that the root-mean-squared of the residual surface pressures P_i is observed to *increase*, rather than decrease), then the correction vector $\Delta_j^{(k)}$ is halved and the iteration (22) is repeated.

Solutions to equations (21) are usually obtained rapidly, due to the quadratic convergence of Newton's method. When $N = 130$, a converged free-surface profile with root-mean-squared surface pressure $< 10^{-10}$ is obtained in four or five iterations, and requires about two minutes

of computing time on a CDC CYBER 173 computer. It is often sufficient to start the iteration with an initially flat profile ($\eta' = 0$), although occasionally, a previously-computed non-linear solution is used for this purpose.

The wave resistance D of the semi-elliptical body is computed from the non-linear free-surface profile using equation (8) to generate values of ξ' at points along the bottom $\psi = 0$. These values are numerically integrated to obtain ξ, using equation (6) to supply the value of ξ at the first point ϕ_0 upstream.

Equations (12) are now solved by cubic-spline interpolation and Newton's method, and the drag D is evaluated from equation (11) using Trapezoidal Rule integration.

5. Presentation of results

When $F^2 < 1$, Lamb's linearized theory predicts a surface profile free of waves on the upstream side, and in general possessing a downstream wave train. For $F^2 > 1$, however, a symmetric, wave-free profile is obtained. These general features are confirmed by the non-linear results. For $F^2 > 1$, the non-linear solution also indicates a symmetric, wave-free profile (see Forbes and Schwartz [4]); however, we consider this branch of solutions possibly to be physically unrealistic, and accordingly, they will not be discussed further in this paper.

In Fig. 2 we present a plot of wave drag D as a function of the ellipse half-length α, for an ellipse of height $\beta = 0.02$ in a stream with $F = 0.8$. The dashed line represents the linearized result, evaluated from equation (16). This is compared with the drag computed from converged non-linear free-surface profiles, obtained for 36 different values of α. For large values of α, the non-linear drag curve exhibits a marked shift to the right, which is in agreement with previously observed trends [2, 3]. In addition, the non-linear drag at the first peak is significantly greater than the linearized value. Note that the non-linear drag is very small indeed at the two minima indicated on the diagram.

In Fig. 3, the extent to which the non-linear downstream wave train may be made to vanish for special choices of α, β, F is investigated. Here, $\beta = 0.02$ and $F = 0.8$, as in Fig. 2. In Fig. 3 we have plotted three non-linear surface profiles; when $\alpha = 1.6$, the downstream wave amplitude,

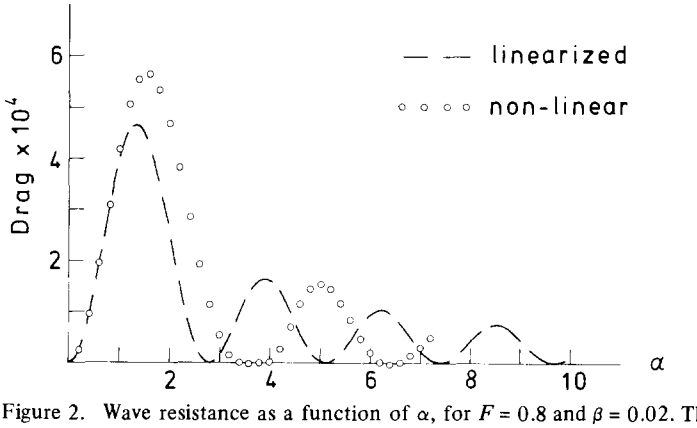

Figure 2. Wave resistance as a function of α, for $F = 0.8$ and $\beta = 0.02$. The dashed line is Lamb's result, and the points indicate results obtained from converged non-linear surface profiles.

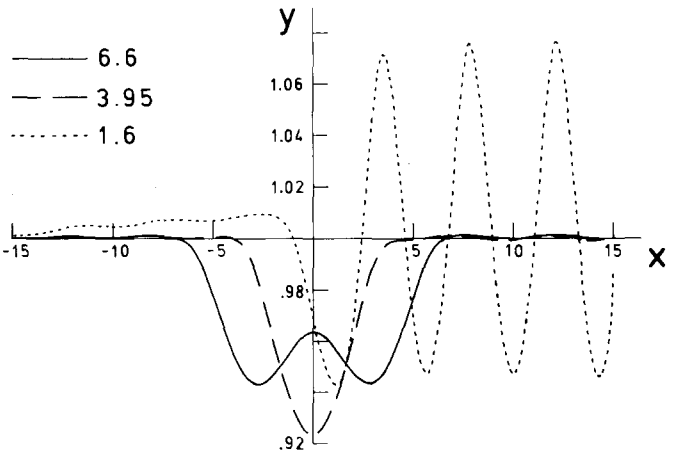

Figure 3. Three free-surface profiles for $F = 0.8$ and $\beta = 0.02$. Results for $\alpha = 1.6$, $\alpha = 3.95$ and $\alpha = 6.6$ are shown.

and hence also the wave drag in Fig. 2, both attain their maximum values, whilst the downstream wave amplitude is at a miminum for $\alpha = 3.95$ and $\alpha = 6.6$. Note that all three surface profiles in Fig. 3 exhibit a very small wave train *upstream* of the semi-ellipse. This is a numerical error due to the truncation of the integrals in equation (9) at $\phi = \phi_0$, and the subsequent imposition of the radiation condition (6) at this point. The reason for the existence of the spurious upstream waves is obvious for the case $\alpha = 1.6$; the imposition of the radiation condition at $\phi = \phi_0$ does not correctly allow for the non-linear rise in the free-surface level ahead of the obstacle (see Benjamin [7]), and consequently, the free surface exhibits a small numerical overshoot in the upstream region. Thus the amplitude of the upstream waves may be reduced somewhat by increasing the value of η_0 slightly above the value given by equation (6), and the size of the upstream waves of the case $\alpha = 1.6$ shown in Fig. 3 has been controlled in precisely this fashion. There is also a numerical error associated with the truncation of the integrals in equation (9) downstream at the last point ϕ_N. The effects of this appear to be localized to a very small region, involving the last quarter wavelength or so downstream, and do not affect the rest of the free-surface profile.

The amplitude of the downstream waves for the cases $\alpha = 3.95$ and $\alpha = 6.6$ shown in Fig. 3 is extremely small, being roughly the same size as the amplitude of the spurious upstream waves. Indeed, we believe that the presence of downstream waves is only due to the existence of the upstream waves, and have no doubt that a surface profile totally without waves may be obtained by adequately eliminating the small, numerically produced, upstream waves. Thus the drag curve of Fig. 2 is expected to pass through zero at $\alpha \sim 3.95$ and again at $\alpha \sim 6.6$. However, the non-linear drag in Fig. 2 actually becomes zero at slightly smaller values of α than these. This is a numerical error in the procedure for computing the non-linear drag (described at the end of Section 4), which is again a consequence of imposing the radiation condition (6) at the point ϕ_0. Thus, although the non-linear drag may be computed without difficulty for small α, the results are more subject to error as α becomes large and F becomes small.

The non-linear effects of the ellipse height β upon the downstream peak-to-trough wave height are investigated in Fig. 4. Results are presented for $\beta = 0.05$ and for $\beta = 0.1$, at $F = 0.5$.

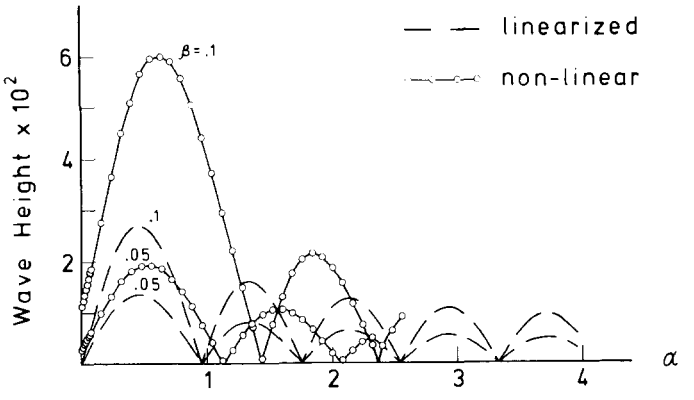

Figure 4. Downstream wave height as a function of α, for $F = 0.5$. Linearized and non-linear results are presented for $\beta = 0.05$ and $\beta = 0.1$. The linearized result is indicated by a dashed line. Points denote non-linear results.

The linearized result was computed from equation (15), whilst in the non-linear case, results were obtained for 36 different values of α when $\beta = 0.05$, and for 39 values of α when $\beta = 0.1$. The wave drag is not shown for these cases, since the error which occurs in the computation of the non-linear wave resistance at large values of α renders the accuracy of the results uncertain.

According to the linearized theory, the values of α at which the wave height becomes zero are functions only of F, and do not depend on β. However, the non-linear results in Fig. 4 show a strong dependence on β. For $\beta = 0.05$, the non-linear wave height takes its first minimum at a value of α which is about 20 per cent larger than the value predicted by linearized theory, and for $\beta = 0.1$, the value of α at which the first minimum occurs is some 50 per cent greater than the linearized result. At this value of the Froude number, surface profiles have again been computed for which the height of the downstream waves is extremely small, and we do not doubt that it may be made to vanish altogether by eliminating the spurious waves from the upstream portion of the flow.

The behaviour of the wave height as $\alpha \to 0$ is also of interest. In this case, the ellipse degenerates to a vertical plate of zero thickness attached to the bottom. Lamb's theory ceases to be valid for small α, and in the limit $\alpha \to 0$, predicts a downstream wave height of zero. This tendency is not observed in the non-linear results; instead, the non-linear wave height appears to remain finite as $\alpha \to 0$. This result is entirely to be expected, since a vertical plate still disturbs the upstream uniform flow, and thus acts as a wave-maker.

6. Remark

In this paper, the effects of non-linearity on the wave resistance experienced by a submerged semi-elliptical body attached to the bottom have been studied, and the numerical results indicate that the non-linear drag should apparently vanish at certain values of the ellipse length. However, although free-surface profiles have been obtained for which the downstream wave height is extremely small, we have not yet observed it to vanish completely, and we believe this

to be due to the necessity of the present method to impose a radiation condition upstream. To search for configurations having exactly zero drag, it may perhaps be possible to formulate the problem differently, taking advantage of the symmetry of the solution about $x = 0$ for these cases, and allowing all the free-surface points to vary. The parameter α would presumably be an unknown quantity, to be obtained along with the free-surface profile in the Newton's method solution of the problem. As with the linearized theory, the non-linear wave drag possibly vanishes for an infinite number of values of α, when β and F are fixed.

7. Acknowledgement

This work was supported by an Australian Commonwealth Postgraduate Research Award.

REFERENCES

[1] H. Lamb, *Hydrodynamics* (6th edition), Cambridge University Press (1932).
[2] L. W. Schwartz, Nonlinear solution for an applied overpressure on a moving stream, *J. Eng. Math.* 15 (1981) 147-156.
[3] C. von Kerczek and N. Salvesen, Nonlinear free-surface effects – the dependence on Froude number, *Proc. 2nd Int. Conf. on Numerical Ship Hydrodynamics* (1977) 292-300.
[4] L. K. Forbes and L. W. Schwartz, Free-surface flow over a semi-circular obstruction, to appear in *J. Fluid Mech.* (1981).
[5] L. K. Forbes, Non-linear free-surface flows about blunt bodies, *Ph.D. Thesis, University of Adelaide* (1981).
[6] J. V. Wehausen and E. V. Laitone, Surface waves, in: *Handbuch der Physik*, vol. 9, Springer-Verlag (1960).
[7] T. B. Benjamin, Upstream influence, *J. Fluid Mech.* 40 (1970) 49-79.